Johann Radon Institute for
Computational and Applied Mathematics
Austrian Academy of Sciences (ÖAW)

Analytical approximation and numerical simulations for periodic travelling water waves

K. Kalimeris

RICAM-Report 2017-28

PHILOSOPHICAL TRANSACTIONS A

rsta.royalsocietypublishing.org

Research

Article submitted to journal

Subject Areas:
Applied Mathematics, Differential Equations, Fluid Mechanics

Keywords:
travelling water waves, vorticity, asymptotic expansions, numerical continuation

Author for correspondence:
Konstantinos Kalimeris
e-mail:
konstantinos.kalimeris@ricam.oeaw.ac.at

THE ROYAL SOCIETY PUBLISHING

Analytical approximation and numerical simulations for periodic travelling water waves

Konstantinos Kalimeris[1]

[1]Radon Institute for Computational and Applied Mathematics, Austrian Academy of Sciences

We present recent analytical and numerical results for two-dimensional periodic travelling water waves with constant vorticity. The analytical approach is based on novel asymptotic expansions. We obtain numerical results in two different ways: the first is based on the solution of a constrained optimization problem, and the second is realized as a numerical continuation algorithm. Both methods are applied on some examples of non-constant vorticity.

1. Introduction

The analysis of the water wave problem dates back to the studies of Newton, with Gerstner [9,27] being the first to consider nonlinear waves; a detailed review on the origins of water wave theory is given in [22], where the main contributions until the great work of Stokes [49] are presented. Since then, an abundance of work has been appeared, using a variety of mathematical formulations of the physical problem and studying analytical, numerical and experimental aspects of the problem. Not in few cases, numerical investigations have guided subsequent rigorous mathematical analysis. Furthermore, a detailed insight may be extracted through a combined application of analytical and numerical approaches, which is not otherwise possible to obtain from either approach in isolation.

In the present work we start from Euler's equations, and by reviewing the methodology of Constantin and Strauss in [18], we derive a mathematical formulation for two dimensional, periodic, travelling water waves with variable vorticity. It is worth pointing out that, while a recent alternative approach for constant vorticity was devised in [20], the methodology in [18] is more adequate for the considerations which are pursued in this paper.

Firstly, by introducing a stream function we formulate the free boundary value problem (2.15), which was rigorously derived in [16]. Consecutively, a partial hodograph transformation yields the nonlinear boundary value problem (3.3); the equivalence of the latter one with the Euler equations is proven in [18]. A key role in the analysis of this problem is the occurrence of a bifurcation parameter which is indicative of the total energy of the wave; this parameter, denoted by Q, is called the hydraulic head of the flow. In [18] it was proven that for a specific value $Q = Q^*$, there exists a bifurcation point on the diagram of the solution. In particular, in the neighbourhood of Q^* and for the same value $Q > Q^*$, the problem (3.3) admits two qualitatively different solutions: the first one corresponds to a laminar flow, and the second one to a water wave with non-vanishing amplitude, a so-called 'genuine wave'. Moreover, the latter waves come as a family, formulating a bifurcating branch.

In the present work we review one analytical and two numerical methods for approximating solutions which belong to the interesting branch of the bifurcation diagram, i.e. solutions that correspond to genuine waves. Furthermore, through a systematic analysis we reconstruct the whole branch of the solution until a limiting solution which was predicted by the analysis in [18], and corresponds to waves of maximal amplitude. It is important to mention that some results obtained from the analytical approach provide the background of the development of these numerical techniques.

In [33] high-order approximations to periodic travelling wave profiles are derived, through a novel expansion. This expansion incorporates the variation of the total mechanical energy of the water wave and yields the extension of these approximations to any finite order. The basic ideas and results of this work are reviewed in section 4, and these expansions are given in equations (4.2) and (4.1). In the absence of flow reversal, the analysis in [15,26] ensures the convergence of the infinite Taylor expansions, due to the analyticity of the streamlines, whereas the available results on regularity for flow reversal are C^∞, see the results in [21]. For the first rigorous constructions of travelling waves occurring, via power series approximations, we refer to the works of Nekrasov [44], Levi-Civita [39], and Struik [51].

The first numerical approach which is reviewed here computes large-amplitude travelling water waves in flows with constant vorticity and is based on a penalization method. The algorithm is realized as a partial differential equation (PDE) constrained optimization formulation, maximizing the wave amplitude subject to the PDE constraint induced by (3.3). This algorithm is quite general, displaying results for some specific cases of non-constant vorticity in [16]. The second computational approach is based on numerical continuation techniques, which are suitably adapted to the water wave problem for obtaining non-laminar flows of constant vorticity and particular cases of vorticity which varies linearly and quadratically with the streamfunction, see [3]. Through this, the bifurcation curve which starts from Q^* and contains non-laminar flows is reconstructed. This procedure is limited by waves that include a stagnation point, i.e. a point where the horizontal velocity of the flow becomes equal to the propagation speed of the wave. Water waves with maximal amplitude are connected with the existence of points of stagnation in their flow. Both these approaches are reviewed in section 5.

Computations which are based on the numerical continuation approach have been performed earlier in [36,37], with several interesting results which agree with the relevant analytical predictions. Among the most important results of those works we point out the following: The stagnation can occur, not only at the crest, but also at the point on the bottom directly below the crest. Along the bifurcation curve, for fixed relative mass flux[1] p_0, the amplitude of the wave is increasing and the depth d varies only slightly. Furthermore, the waves of maximal amplitude are obtained at the end of the bifurcation curve and the maximal amplitude is an increasing function of $|p_0|$, in the case of constant vorticity. Finally, the shapes of the streamlines of the extreme waves depend on the vorticity, which is a result observed also in several numerical works and indicates the importance of the effect that the vorticity has on the features of water waves.

[1]The flux p_0 is defined in (2.8).

One important aspect of the formulation (3.3) is that once a solution is found, then one can readily obtain other important features of the flow, such as the velocity vector and the pressure on the flat bottom. In several instances of this work we illustrate these flow characteristics, derived either from analytical or numerical approaches, for several different types of wave-current interactions. Laboratory experiments and numerical simulations for irrotational waves are discussed in [4,5,31,54], while this type of studies for wave-current interactions in flows of constant vorticity were pursued in [10,23,36,37,52,53]. In a number of recent works, waves with critical layers are studied numerically, see for example [46,48].

2. Mathematical Formulation

(a) Mathematical modelling

We discuss two dimensional, periodic waves with general vorticity and large amplitude. We assume that the water is incompressible and inviscid without surface tension, lies over a flat bottom and is acted upon by gravity g. Moreover we study waves travelling at constant speed and without change of shape at the surface of a layer of water. In this formulation we make no shallowness or small amplitude approximation.

In particular, the water waves have the following properties:

- *Two dimensional:* The motion is identical in any direction parallel to the crest line. Thus, we analyse a cross section of the flow that is perpendicular to the wave crests, choosing appropriate Cartesian coordinates (X, Y). Let the cross-section of the fluid domain be of the form
$$\mathcal{D}(t) = \big\{(X, Y) : X \in \mathbb{R} \text{ and } -d < Y < \xi(t, X)\big\},$$
$d > 0$ is the average depth and ξ is the free surface.
- *Incompresible:* Let $\big(U(t, X, Y), V(t, X, Y)\big)$ be the velocity field. The constant density flow implies the equation of mass conservation
$$U_X + V_Y = 0. \tag{2.1}$$
- *Inviscid:* Let $P(X, Y, t)$ be the fluid pressure. The Euler equations take the form
$$\begin{aligned} U_t + UU_X + VU_Y &= -P_X, \\ V_t + UV_X + VV_Y &= -P_Y - g, \end{aligned} \tag{2.2}$$
where P is the pressure and g is the gravitational constant.
- *Flat bottom:* In its undisturbed state (no waves) the equation of the flat surface is $Y = 0$, and the flat bottom is given by $Y = -d$ for some $d > 0$, i.e. d represents the average depth. Moreover, the flow does not penetrate the horizontal bottom which is given by the boundary condition
$$V = 0, \text{ on } Y = -d. \tag{2.3}$$
- *Free water surface:* Let $Y = \xi(t, X)$ be the free surface for which the same particles always form this surface and this is expressed by
$$V = \xi_t + U\xi_X \text{ on } Y = \xi(t, X). \tag{2.4}$$
- *No surface tension:* The motion of the water and the air is decoupled and this is translated to the condition that the pressure P is equal to the atmospheric pressure P_{atm} on the free surface.

Moreover, we discuss water waves that are *travelling* at constant speed $c > 0$. This has a two-fold meaning: First, in this regime, the free surface is a graph; for irrotational travelling waves see the considerations in [55]. Second, the space-time dependence of the free surface, of the pressure, and of the velocity field has the form $(X - ct)$, i.e. for $(x, y) = (X - ct, Y)$ we have that

- $U(X,Y,t) = u(x,y)$
- $V(X,Y,t) = v(x,y)$
- $P(X,Y,t) = \mathsf{P}(x,y)$
- $\xi(X,t) = \eta(x)$.

Obviously, this change of variables transforms accordingly the Euler equations and the relevant boundary conditions.

Restricting our attention to waves which are *periodic* in x, and taking, for convenience, the length scale to be 2π, we obtain that the velocity field (u,v), the pressure P and the free boundary η are 2π-periodic functions.

Consequently, in a frame moving at the (constant) wave speed, the boundary value problem is defined in the two-dimensional bounded domain

$$\mathcal{D} = \{(x,y) : -\pi < x < \pi \text{ and } -d < y < \eta(x)\}\,,$$

bounded above by the free surface profile

$$S = \{(x,y) : -\pi < x < \pi \text{ and } y = \eta(x)\}\,,$$

and below by the flat bed

$$B = \{(x,y) : -\pi < x < \pi \text{ and } y = -d\}\,.$$

Since d represents the average depth, the waves oscillate around the flat free surface $y = 0$, that is

$$\int_{-\pi}^{\pi} \eta(x)\,dx = 0. \tag{2.5}$$

One may think that the above-mentioned assumptions will significantly restrict the amount of water waves that can be described by this model. However, this is a realistic model for large families of waves which display a plethora of different characteristics, see the relevant discussion in [50] and [18].

An essential flow characteristic is the vorticity

$$\gamma := u_y - v_x, \tag{2.6}$$

which is indicative of underlying currents. With respect to the flow beneath the waves, we restrict our attention to flows for which

$$u < c \quad \text{throughout the fluid.} \tag{2.7}$$

This condition prevents the appearance of stagnation points in the flow and the occurrence of flow-reversals.

(b) Free Boundary Value Problem

A flow characteristic that is necessary for the definition of the free Boundary Value Problem is the *relative mass flux*

$$p_0 = \int_{-d}^{\eta(x)} \big(u(x,y) - c\big)\,dy < 0, \tag{2.8}$$

which is independent of x, see [16]. We introduce the stream function $\psi(x,y)$ as the unique solution of the differential equations

$$\psi_x = -v, \qquad \psi_y = u - c \text{ in } \overline{\mathcal{D}}\,, \tag{2.9}$$

subject to

$$\psi(x,-d) = -p_0\,. \tag{2.10}$$

Note that $\psi(x,y)$ is periodic in the x-variable, and that the constraint (2.10) is consistent with the flat bottom boundary condition (2.3) . Moreover, (2.9) and the definition of vorticity yield

$$\Delta\psi = \gamma \text{ in } \mathcal{D}\,. \tag{2.11}$$

The free boundary condition (2.4) is equivalent to ψ being constant on S, while (2.8) together with (2.10) ensure that this constant must vanish, that is,

$$\psi = 0 \text{ on } S\,. \tag{2.12}$$

On the other hand, due to (2.9), we see that we can re-express, through integration, the mass conservation (2.1) and the Euler equations in (2.2) by the expression

$$\mathcal{B}_B[\psi] := \frac{|\nabla\psi|^2}{2} + g\eta - Q = 0 \quad \text{on} \quad S, \tag{2.13}$$

where Q is a constant called the hydraulic head, which is given by

$$Q = E - P_{atm}, \tag{2.14}$$

with E being a constant which represents the total mechanical energy throughout the flow.

Remark 1. *For two-dimensional travelling water waves, if condition (2.7) holds, then vorticity is necessarily a function of the streamfunction, that is, $\gamma = \gamma(\psi) = \gamma(-p)$, cf. [10].*

Following this concept, in the instances where vorticity is non-constant in this work, we refer to its particular dependence on the streamfunction, see for example the term 'linear vorticity' in Section 5.

The previous considerations show that the governing equations can be formulated in terms of the stream function as the free-boundary problem:

Definition 1. *The constants g (gravitational constant), p_0 (relative mass flux), Q (hydraulic head) and the function $\gamma : [0, -p_0] \mapsto \mathbb{R}$ (vorticity) are given.*

Moreover, for given η, which we assume to be normalized by (2.5), let $\psi = \psi[\eta]$ be the even and 2π-periodic (in the x-variable) solution of the linear equation (2.11) with boundary conditions (2.10) and (2.12).

For given η, this linear *partial differential equation is overdetermined by imposing the non-linear boundary condition (2.13) on S.*

The free boundary problem consists in using the over-determinacy to determine η.

The free boundary value problem can also be viewed as solving an operator equation

$$\mathcal{G}(\eta) = 0\,, \tag{2.15}$$

where $\mathcal{G} : \eta \mapsto \mathcal{B}_B[\psi[\eta]]$.

Evenness of ψ reflects the requirement that u and η are symmetric while v is antisymmetric about the crest line $x = 0$; here, we shift the moving frame to ensure that the wave crest is located at $x = 0$. Symmetric waves present these features and it is known that a solution with a free surface S that is monotone between crest and trough has to be symmetric, see [13,14].

3. A non-linear boundary value problem

Starting from the free boundary formulation of travelling water waves which was derived by the Euler equations in the above section, we apply the Dubreil-Jacotin transformation, introduced

in [25]. This is a partial hodograph transformation, which is described as follows (see Figure 1)

$$q = x, \qquad p = -\psi,$$

and transforms the unknown domain $\mathcal{D}$ to the rectangle

$$R = \{(q,p) : \ -\pi < q < \pi \,, \ p_0 < p < 0\}. \tag{3.1}$$

Let

$$h(q,p) = y + d \tag{3.2}$$

be the height above the flat bottom B. Since ψ is a strictly decreasing function of y, for every fixed x the height h above the flat bottom is a single valued function of ψ (equivalently, of p).

Consequently, through the methodology in [16,18], the free boundary problem defined by (2.15) takes the form of the following second order elliptic non-linear fixed boundary value problem for the even (in q) function $h(q,p)$:

$$\begin{aligned} &\mathcal{H}[h] := (1+h_q^2)h_{pp} - 2h_p h_q h_{pq} + h_p^2 h_{qq} - \gamma h_p^3 = 0 \ \text{ on } \ R\,, \\ &\mathcal{B}_0[h] := 1 + h_q^2(q,0) + \big(2gh(q,0) - Q\big)h_p^2(q,0) = 0\,, \\ &\mathcal{B}_1[h] := h(q,p_0) = 0\,, \end{aligned} \tag{3.3}$$

where R is given by (3.1), γ is the given vorticity, g is the gravitational constant and Q is given in (2.14), being indicative of the total mechanical energy of the wave. Moreover, the free boundary $\eta(x)$ is given by $h(q,0) = \eta(x) + d$, for an average depth d.

Remark 2. *The average depth of the fluid can only be recovered a posteriori from the height-function by taking the mean integral of $h(q,0)$ over a period and using relation (2.5).*

A novel approach to overcome this issue was initiated in [28,29], where an alternative bifurcation approach which fixes the mean-depth a priori is presented, see also [47]. Based on this formulation one may proceed in a similar way both in the analytical and numerical aspects in order to compute families of non-laminar water waves of fixed depth, where the relative mass flux p_0 will be varying. We consider this a very fruitful approach in order to see, among other interesting features, how the variation of the quantity p_0 will affect important characteristics of waves. For a brief overview on the influence of p_0 on the wave characteristics we refer to [3].

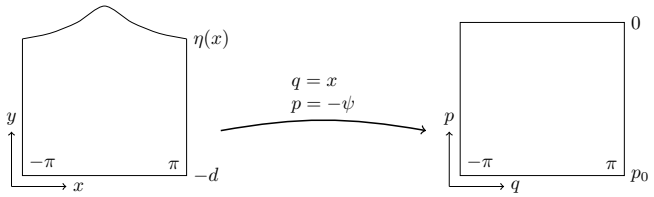

Figure 1: Dubreil-Jacotin transformation

In this formulation the parameter Q is treated as a bifurcation parameter. In order to make clear this statement, we first have to discuss some specific solutions of the problem (3.3).

(a) Laminar solutions

The laminar flows are readily obtained as the q independent solutions of (3.3) by the following formula

$$H(p;\lambda) = \int_{p_0}^{p} \frac{ds}{\sqrt{\lambda - 2\Gamma(s)}}, \quad p_0 \le p \le 0\,, \tag{3.4}$$

provided that the parameter $\lambda > 0$ satisfies the equation

$$Q = \lambda + 2g \int_{p_0}^{0} \frac{ds}{\sqrt{\lambda - 2\Gamma(s)}}\,, \tag{3.5}$$

where $\Gamma(s) = \int_0^s \gamma(-p)dp$.

(b) Bifurcation and linearised solution

Initially we restrict our attention to the case of constant vorticity, i.e. γ=constant. For $\gamma = 0$ we obtain the irrotational waves, which have as a limiting case the so-called Stokes' wave of greatest height. Moreover, the case $\gamma \neq 0$ gives rise to a large number of rotational waves, which display a variety of different characteristics. This mechanism describes waves where wave-current interactions cause significant increase of the wave amplitude in little time; such a case appears at the Columbia River entrance, where tidal currents cause a doubling in the wave height, see [32,35].

In the case of constant vorticity, i.e. γ=constant, apart from the laminar flows one can obtain the solution of the linearised problem. In this case the Boundary Value Problem (BVP) (3.3) is linearised around the laminar flow $H(p;\lambda)$ and gives a linear separable PDE and a Robin boundary condition. For some specific value λ^* (equivalently Q^*) an existence result for the solution of this BVP is presented in [18]. Moreover, the linearised solution is given by

$$m(q,p) = \frac{\sqrt{\lambda_* - 2\gamma p_0}}{\sqrt{\lambda_* - 2\gamma p}} \sinh\left(\frac{2(p-p_0)}{\sqrt{\lambda_* - 2\gamma p} + \sqrt{\lambda_* - 2\gamma p_0}}\right) \cos q, \tag{3.6}$$

where $\lambda_* > 0$ is the solution of the dispersion relation

$$\frac{\lambda}{g - \gamma\sqrt{\lambda}} + \tanh\left(\frac{2p_0}{\sqrt{\lambda} + \sqrt{\lambda - 2p_0\gamma}}\right) = 0. \tag{3.7}$$

Equations (3.4) and (3.5) are now simplified to

$$H^*(p) = \frac{2(p-p_0)}{\sqrt{\lambda_* - 2\gamma p} + \sqrt{\lambda_* - 2\gamma p_0}}\,, \quad p_0 \le p \le 0. \tag{3.8}$$

and

$$Q^* = \lambda_* + \frac{4g|p_0|}{\sqrt{\lambda_*} + \sqrt{\lambda_* - 2\gamma p_0}}, \tag{3.9}$$

respectively, with λ_* satisfying the dispersion equation (3.7).

It was shown in [18] that the point (Q^*, H^*) is a bifurcation point in the parameter space, see Figure 2. In brief, near the laminar flows (3.4), as the parameter λ varies, there are generally no genuine waves, except at critical values $\lambda = \lambda^*$ which is determined by the dispersion relation (3.7). Near this bifurcating laminar flow H^*, we have two solution curves: one laminar solution curve $\lambda \mapsto H(p;\lambda)$, where λ and Q are related by (3.5), and one non-laminar solution curve $Q \mapsto h(q,p;Q)$ such that $h_q \not\equiv 0$ unless $h = H^*$, see Figure 2. In [18] it was shown that the curve containing the non-laminar solutions can be extended to a global continuum $\mathcal{C}$ that contains solutions of (3.3) with $\frac{1}{h_p(q_s,p_s)} \to 0$ at some (q_s,p_s). This condition is characteristic of flows whose horizontal velocity u is arbitrarily close to the speed c of the reference frame, at some point in the fluid, the limiting configuration being a flow with stagnation points.

In what follows we start from the results produced by this analysis and we obtain general methods, for approximating solutions of (3.3) that correspond to flows of large amplitude.

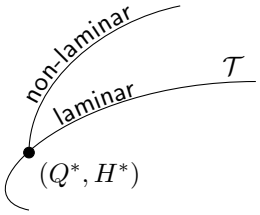

Figure 2: Bifurcation diagram

Firstly, we interpret the function

$$\hat{h}(q,p;b) = H^*(p) + b\, m(q,p), \tag{3.10}$$

as a perturbation of a laminar solution of the system (3.3), in the following sense

$$\mathcal{H}[\hat{h}](q,p) = \mathcal{O}(b^2)\,,\ \mathcal{B}_0[\hat{h}](q) = \mathcal{O}(b^2) \text{ and } \mathcal{B}_1[\hat{h}](q) = 0 \tag{3.11}$$

and that the amplitude of the water wave is of order $\mathcal{O}(b)$. Having in mind that the wave amplitude vanishes for the laminar flows, we can see the expression (3.10) as an approximation of small amplitude water waves. Thus, the expression given in (3.10) may serve as an initial step in iterative numerical procedures for computing waves of large amplitude. Two different such approaches are described in section 5.

Secondly, we can see this expression as the first order asymptotic expansion of a general solution of the BVP (3.3) which represents a large amplitude water wave. This point of view on this expression is triggered by the bifurcation argument which was described above and was proved in [18]. A rigorous construction of the full asymptotic expansion is presented in [33]. Higher order expansions result in waves of large amplitude; this analytical approximation of genuine waves is presented in section 4.

4. Analytical approximation

The analytical approach starts from the perturbation of a laminar solution around the bifurcation point described above. The location of the bifurcation point and the direction of this perturbation are given by (3.8) and (3.9) and determined as the solution of an eigenvalue problem described in [18]. Then, asymptotic techniques are applied in order to approximate genuine water waves, i.e. solutions of (3.3) that correspond to non-laminar flows. This idea is introduced in [17] and analysed in [33], in order to approximate the bifurcation branches in the solution diagram, Figure 2. Developing this idea, in [33] we are able to derive explicit formulae for families of water waves contained in the bifurcation branch of non-laminar flows. Some of the results related with important characteristics of the waves are depicted in Figure 3. In particular, the free surface, and the pressure of the water at the bottom are depicted for different values of constant vorticity; the latter characteristic is particularly important, since in practice the state of the sea surface is often gathered from the knowledge of subsurface pressure [6,7,11,28,38,45]. The knowledge of these flow characteristics is very useful in qualitative studies, see [8,19]. The latter works are particularly noteworthy since the qualitative studies contained therein relate to the fully-nonlinear exact governing equations; in this context we also refer to [12,30,40,41]

Using the above "bifurcation argument" we observe that the variation of the parameter Q (the hydraulic head of the flow) about the uniquely determined value Q^* induces an approximation of non-laminar flows, in the following sense:

Definition 2. *Define the approximation for the hydraulic head of the flow,*

$$Q \approx Q^{(2N)}(b) = Q^* + \sum_{k=1}^{N} Q_{2k} b^{2k}, \qquad b \in \mathbb{R}. \tag{4.1}$$

Definition 3. *Define the approximation for the height function $h(q,p;Q)$,*

$$h(q,p;Q) \approx h^{(2N+1)}(q,p;b) = \sum_{n=0}^{2N+1} h_n(q,p) b^n, \tag{4.2}$$

with

$$h_{2k}(q,p) = \sum_{m=0}^{k} \cos(2mq) f_{2m}^{2k}(p) \tag{4.3}$$

and

$$h_{2k+1}(q,p) = \sum_{m=0}^{k} \cos((2m+1)q) f_{2m+1}^{2k+1}(p), \tag{4.4}$$

where $f_0^0(p) = H(p;\lambda_*)$.

Our goal is to *simultaneously* determine the functions $\{h_n(q,p)\}_{n=1}^{2N+1}$ and the constants $\{Q_{2k}\}_{k=1}^{N}$ so that the system (3.3) be satisfied up to order b^{2N+2}, i.e.,

$$\begin{aligned} &\mathcal{H}[h^{(2N+1)}](q,p) = \mathcal{O}(b^{2N+2}), \\ &\mathcal{B}_0[h^{(2N+1)}](q) = \mathcal{O}(b^{2N+2}) \quad \text{and} \quad \mathcal{B}_1[h^{(2N+1)}](q) = 0. \end{aligned} \tag{4.5}$$

The fact that the asymptotic expansion $h^{(2N+1)}$ is an approximation of a non-laminar wave is established by the following theorem, which has a central role in the current analysis of the water wave problem, and is stated and proved in [33].

Theorem. *Let g, p_0, γ be fixed, λ_* be defined as the solution of (3.7) and Q^* given by (3.5).*

There exist specific sets of functions $\{h_n(q,p)\}_{n=1}^{2N+1}$ and constants $\{Q_{2k}\}_{k=1}^{N}$, such that the function $h^{(2N+1)}(q,p;b)$ defined in (4.2) satisfies the system (4.5), under the constraint that the hydraulic head Q is given by (4.1).

Furthermore, the details of the proof presented in [33], suggest that the Theorem is true for a larger class of vorticities. This class is described through an appropriate change of variables, which reduces the complexity of the proof to the one for the constant vorticity case; for candidate member of this class we refer to [34,42,43].

The above theorem implies that the dominant term of the wave height of this approximation of the water wave is of order b, i.e,

$$\begin{aligned} a^{(N)} &= h^{(2N+1)}(0,0;b) - h^{(2N+1)}(\pi,0;b) \\ &= b\,[h_1(0,0) - h_1(\pi,0)] + \mathcal{O}(b^2) = 2b f_1^1(0) + \mathcal{O}(b^2). \end{aligned} \tag{4.6}$$

This condition indicates the accuracy of approximation of genuine waves in the following sense: Equations (4.5) show that $h^{(2N+1)}$ is an approximation of a solution up to order b^{2N+2}, whereas the relation (4.6) shows that $h^{(2N+1)}$ differs from the laminar solution at order b. Consequently, $h^{(2N+1)}$ is 'closer' to a non-laminar solution. An illustration of this is given in Figure 4, for a fixed relative error.

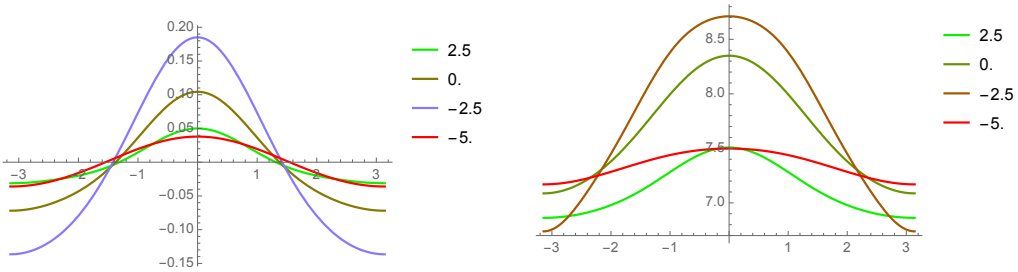

(a) The free surface $\eta(x)$.

(b) The water pressure on the flat bottom B.

Figure 3: Characteristics of the waves for different values of the vorticity.

For the explicit formulae of higher order expansions we refer to [33]; fixing the values of the parameters

$$g = 9.8, \quad \text{and} \quad p_0 = -2, \tag{4.7}$$

we depict these expansions for the irrotational case, up to the fifth order, in Figure 4. More complicated formulae for the case of constant vorticity are provided in [33], which we avoid to present here for matters of brevity; the illustration of some examples are given in Figure 3.

Finally, the proof of the Theorem in [33], being constructive, provides a deterministic algorithm for computing water waves of maximal amplitude. The realisation of such an algorithm for the computation of water waves in this class of vorticities is a work under progress [2].

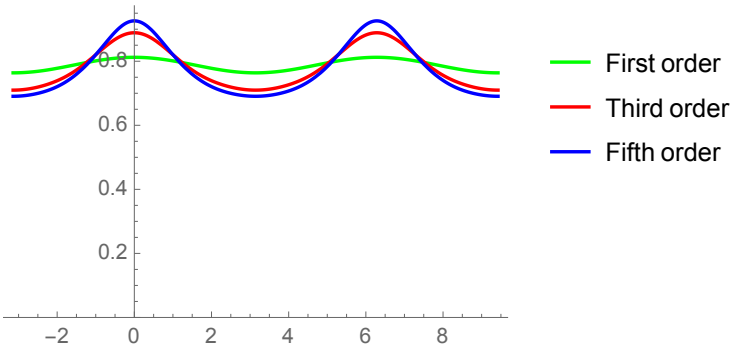

Figure 4: The free surface $h(q, 0)$ for expansions of different orders.

5. Computational approaches

Below we discuss two iterative methods for computing water waves of large amplitude, following the numerical treatment performed in [3,16], obtaining several interesting results which agree with the relevant analytical predictions. We point out that the initial guess for these iterative schemes is of great importance, so that our algorithms select the branch of the bifurcation diagram containing non-laminar flows. Low order expansions arising from (4.2) are suitable for providing this initial guess.

(a) A penalization method

In [16], for the selection of waves of large amplitude we impose the constraint of maximization of the norm of the slope of the wave profile, over one wavelength. A penalization method to solve numerically this constrained optimization problem in the fixed rectangular domain R, given in (3.1), is proposed. The main point is the minimization of the quantity

$$\mathcal{E}[h] := -\int_R h_q^2\,,$$

subject to the PDE constraint that h satisfies (3.3).

The energy function $\mathcal{E}$ is chosen in such a way that it vanishes for laminar flows (in which $h_q \equiv 0$), thus selecting genuine waves. This permits us to provide accurate simulations of the surface water wave, but also of the main flow characteristics (fluid velocity components, pressure) beneath it.

A brief description of the algorithm, which implements the penalization method, is given below:

(i) *Initialize* $k = 0$*:* Choose a constant $\nu_0 > 0$ (typically small). Use an initial guess $h^{(0)}$ of the solution of (3.3), by selecting $h^{(0)}(q,p) = \hat{h}(q,p;b)$ from (3.10). These forms guarantee that (3.11) holds.

(ii) $k \to k+1$: Given $h^{(k)}$ we solve the linear equation for h, obtained by (3.3) when freezing the coefficients of lower order from the previous iteration step. The solution is denoted by $h^{(k+1)}$.

(iii) *Compute* $h_p^{(k+1)}$. Because we work with a semi implicit scheme we have to use a relative small step-size, which is determined here.

- If $h_p^{(k+1)} > 0$ then put $\nu_{k+1} = \nu_k$ and update $h^{(k+2)}(q,p) = h^{(k+1)}(q,p) + \nu_{k+1} h_{qq}^{(k+1)}(q,p)$. We emphasize that $h_{qq}^{(k+1)}$ is the steepest descent energy of the quadratic functional $\mathcal{E}$. From this perspective we might call this algorithm a *steepest descent* algorithm.
- else put $\nu_{k+1} = 0$ and update

$$h^{(k+2)}(q,p) = F(p) - h^{(k)}(q,p).$$

The function F is given by $F(p) \simeq 2H(p,\lambda^*)$.

(iv) Among the stopping criteria of the algorithm is the satisfaction of the system of equations (3.3) up to small error. If the algorithm is not terminated then move to the second step.

The different branches of the third step guarantee that the residuals of the boundary conditions and the differential equations are decreasing. More details on the realisation of the algorithm, as well as the justification of this realisation are presented in [16]. In Figure 5 we present the basic results for the irrotational case, considering the wave profile and the velocity field. This algorithm is general in the sense that we obtain results for other cases of vorticity, with some results for constant and linear cases being presented in [16]. Here, we will illustrate results of this more general case, through the more sophisticated approach which is presented in the following subsection.

(b) A numerical continuation technique

In this section, we describe a numerical continuation approach for computing water waves of large amplitude, through the mathematical formulation which is given by (3.3). Appropriate techniques are applied in order to overcome some particular obstacles of the problem related with the appearance of turning points, bifurcating points and stagnation points. As a result, the induced algorithm in [3] is efficient and not expensive. Additionally, it uncovers new parts of the interesting branch of the bifurcation diagram, i.e. families of waves with novel characteristics.

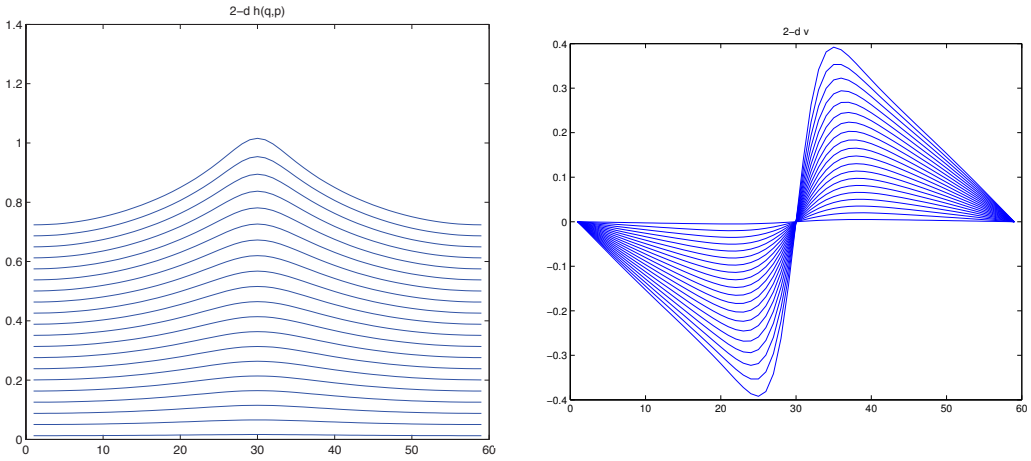

(a) $h(q,p)$ (b) $v(q,p)$

Figure 5: The height $h(q,p)$ of the streamlines and the vertical fluid velocity $v(q,p)$ along streamlines, depicted for the irrotational case $\gamma = 0$. The q-axis is discretized into segments of length $2\pi/60$.

This algorithm, at its limiting point, computes water waves near stagnation; a family of such waves is depicted in Figure 6. Furthermore, these numerical results agree with the ones in the literature (see [36,37]), and have a somewhat improved accuracy, which in some cases is important enough to give an additional understanding of the solutions of the problem. Finally, the generality of this algorithm is established by the computation of some cases of continuous and non-constant vorticity.

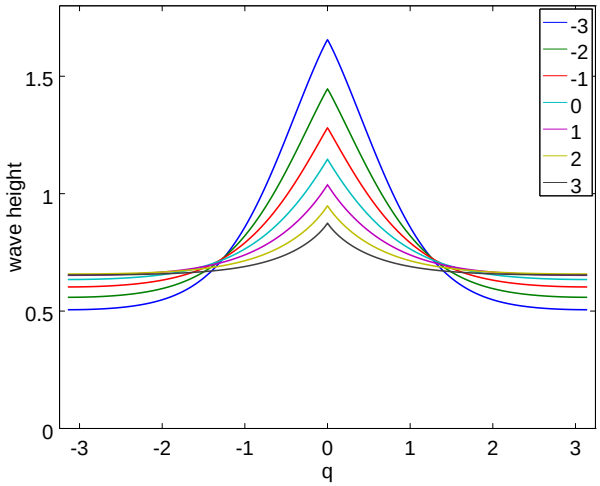

Figure 6: Wave profile for different values of constant vorticity.

(i) Predictor Corrector method

Discretization of (3.3) leads to a system of nonlinear equations

$$F(\theta, \mathbf{h}) = \mathbf{0} \tag{5.1}$$

with a given mapping $F : \mathbb{R} \times \mathbb{R}^N \to \mathbb{R}^N$ and unknowns $\mathbf{h} \in \mathbb{R}^N$ and $\theta \in \mathbb{R}$. To overcome the two major problems in solving (5.1), the underdetermined system and the need for a good initial guess, we employ a numerical continuation strategy. We consider the case that at least one solution is known and the goal is to compute additional solutions. Parametrization of the solution curve and fixing the step size results in a well defined problem and the known solutions are used to predict an initial guess. As corrector we use a Newton algorithm to solve the system of nonlinear equations. Below we give a short introduction into this topic; for a more elaborated study we refer to [1,24].

Let $\mathcal{C}$ be the set of all pairs satisfying (5.1) and $(\theta_k, \mathbf{h}_k) \in \mathcal{C}$ a known solution, then the problem is to find a new solution

$$F(\theta_{k+1}, \mathbf{h}_{k+1}) = \mathbf{0}.$$

Since this is a underdetermined system we first have to find an additional equation. Assume that a parametrization of the solution curve $\mathcal{C}$ in a neighborhood of $(\theta_k, \mathbf{h}_k)$ is given by the equation $p(\theta, \mathbf{h}, s) = 0$. Then for a fixed step size s we obtain the following system.

$$\begin{pmatrix} F(\theta_{k+1}, \mathbf{h}_{k+1}) \\ p(\theta_{k+1}, \mathbf{h}_{k+1}, s) \end{pmatrix} = \begin{pmatrix} \mathbf{0} \\ 0 \end{pmatrix}. \tag{5.2}$$

The existence and uniqueness of a solution to (5.2) depends on the choice of p and the solution set $\mathcal{C}$. In [3] we make the following two choices for p:

- The natural parametrization which corresponds to fixing the value of θ and is given by
$$p(\theta, \mathbf{h}, s) = \theta - (\theta_k + s). \tag{5.3}$$
- The local parametrization, where instead of θ we can choose any entry of $\mathbf{h}$ as parameter. Let i be an index of $\mathbf{h}$; this parametrization is given by
$$p(\theta, \mathbf{h}, s) = \mathbf{h}[i] - (\mathbf{h}_k[i] + s).$$

Figure 7 shows both these parametrizations on a bifurcation diagram that plots $(\theta, \mathbf{h}[i])$ for all solutions in $\mathcal{C}$. Additionally to $\mathcal{C}$ the line of all pairs $(\theta, \mathbf{h})$ satisfying $p(\theta, \mathbf{h}, s) = 0$ is also plotted, the solution we seek is the intersection of these two lines. The existence and uniqueness of such an intersection depends on $\mathcal{C}$ and the choice of s. In the example, $\mathcal{C}$ has a turning point in θ, so it exists no solution pair that satisfies the natural parametrization if s is too large. Indeed, if the current solution is exactly on the turning point, it exists no $s_0 > 0$ such that (5.3) describes a parametrization of $\mathcal{C}$. In such a case, one way to proceed with the numerical continuation is by parametrizing with respect to another characteristic such that the bifurcation curve does not have a turning point; in the given example this is $\mathbf{h}[i]$.

For our model problem (3.3) it proved most effective to parametrize by the entry of $\mathbf{h}$ corresponding to the highest point of the wave.

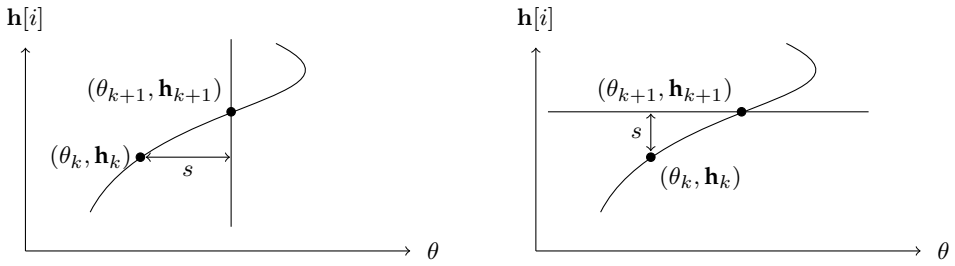

Figure 7: Natural and local parametrization

The predictor is the initial guess for the Newton scheme and will be denoted as $(\theta_{k+1}^{(0)}, \mathbf{h}_{k+1}^{(0)})$. Of the many predictors described in literature we only briefly introduce two, the trivial and secant predictor

$$(\theta_{k+1}^{(0)}, \mathbf{h}_{k+1}^{(0)}) := (\theta_k + s^{(0)}, \mathbf{h}_k),$$
$$(\theta_{k+1}^{(0)}, \mathbf{h}_{k+1}^{(0)}) := (\theta_k, \mathbf{h}_k) + s^{(0)}(\theta_k - \theta_{k-1}, \mathbf{h}_k - \mathbf{h}_{k-1}).$$

The value $s^{(0)}$ is chosen such that the parametrization equation is satisfied.

(ii) Constant vorticity

Let b be fixed, then $\hat{h}$ which is given in (3.10), is a predictor for a solution on the bifurcation branch. Note that a too small b will urge the corrector to converge to a laminar wave while a too big b can result in a diverging corrector step. In our experience, the choice $b = s$ with a small enough s leads to convergence to the nonlaminar branch. Efficient predictors are also higher order asymptotic expansions given by (4.2).

The natural choice for the bifurcation parameter θ is Q, which is indicative of the total mechanical energy of the wave, and we assume all other parameters to be fixed, see for example (4.7). While for most of our computations we used Q as the continuation parameter, we note that for waves of constant vorticity we can alternatively fix Q and choose γ to be the continuation parameter. This choice can be beneficial for overcoming some limitations of this approach and compute waves which belong to new parts of the bifurcation curve.

Considering the validation of our algorithm, in [3] we have illustrated the performance of the corrector step to solve (5.2), for which we employ a Newton algorithm. Furthermore, we have performed the same error tests on examples, for which we have the a priori knowledge of the analytical expression of the solution.

The computed waves in this section demonstrate different characteristics below and above a critical vorticity which is $\gamma_{\text{crit}} \approx -2.971$, for the choice of parameters given in (4.7). We emphasize the fact that we obtain, also, some new qualitative results, compared with [36].

The appearance of two turning points in Q and an monotonously increasing wave height along the solution curve is observed for all constant vorticities which are larger than γ_{crit}. The value of γ does have a significant influence on the stagnating waves. Indeed, the results presented in Figure 6 display the following characteristics for the wave profile:

- The wave height decreases, as the vorticity γ gets larger.
- The shape of the wave changes with the vorticity; the crest becomes sharper and the trough wider and flatter as the vorticity increases.

The above procedure does not compute a maximal wave with a sharp angle at the top for all constant vorticities. In particular, if the vorticity is below γ_{crit}, it breaks down earlier; this behaviour was also observed in [36,37] and attributed to a stagnation point at the bottom of the wave. In [3] we modify the above approach: We consider some γ_0 above the critical value and compute the solution with maximum value of Q along the bifurcation curve $\mathcal{C}_{\gamma_0}$. Then we fix Q and instead consider γ as the bifurcation parameter, looking for a solution for $\gamma_1 < \gamma_{\text{crit}} < \gamma_0$. Now we switch back to Q as the bifurcation parameter and compute the upper section of $\mathcal{C}_{\gamma_1}$, bounded above by the wave of maximal wave height and below by the wave with the stagnation point at the bottom. The last wave we could compute was at $\gamma = \gamma_\ell = -3.062$. Numerical experiments show that this approach works and that waves with stagnation point at the top exist even for vorticities below the critical value, see Figure 8.

In summary, the γ-continuation technique in the interval $(\gamma_\ell, \gamma_{\text{crit}})$, indicates the existence of waves that have a stagnation point on the free surface, for vorticities *below* the critical value and conjectures the existence of waves with stagnation points both at the crest and at the bottom, right below the crest. We emphasise the fact that the pressure of the fluid displays a qualitative change for values of vorticity smaller than the critical value. Indeed, in Figure 9a, where we depict the

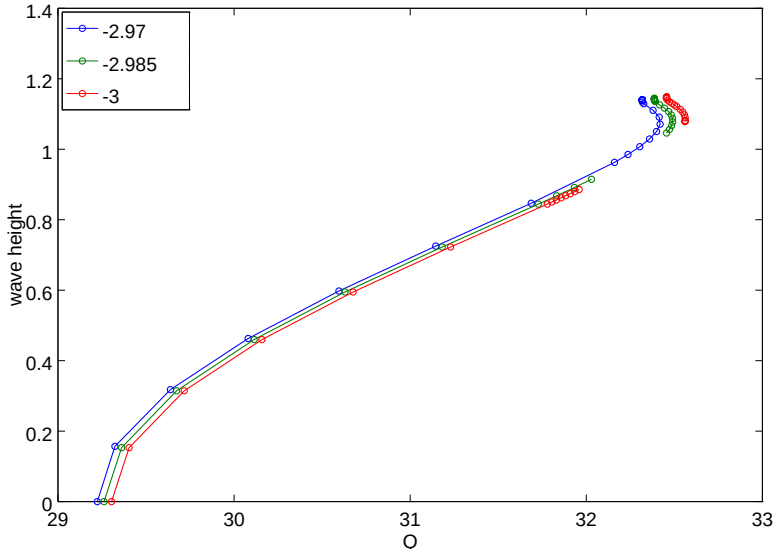

Figure 8: Bifurcation diagram for different values of constant vorticity in the interval $(\gamma_\ell, \gamma_{\text{crit}}]$.

pressure of the fluid at the bottom, we see that when $\gamma < \gamma_{\text{crit}}$, the pressure at the point right below the crest displays a 'plateau' behaviour instead of a local maximum, which characterizes flows with $\gamma > \gamma_{\text{crit}}$.

The former behaviour is more transparent in Figure 9b. Considering the point of the bifurcation curve for which this 'plateau' behaviour of the pressure is more distinct, we make the following three observations: First, for $\gamma = \gamma_{\text{crit}}$, this takes place at the neighbourhood of the point on the bifurcation curve where the gap will appear, namely Q_G. Second, if $\gamma_\ell < \gamma < \gamma_{\text{crit}}$, then this behaviour occurs for the two substantially different waves, which correspond to the endpoints of the gap in the bifurcation curve. Third, if $\gamma < \gamma_\ell$, then this behaviour occurs at the last computable wave.

For a more detailed analysis of the characteristics (including pressure) of the waves corresponding to points around the gap on the bifurcation curve, we refer to [3].

Remark 3. *We find worth noting that the distribution of the pressure in the bulk of the fluid could take substantially different form, depending on the co-ordinate system used for the studying of the problem. An illustrative example is presented in Figure 10, for $\gamma = \gamma_{crit}$ and $Q = Q_G$: In the left picture the level curves of the pressure are drawn in in the physical domain, i.e. for the (x, y)-variables, whereas in the right picture this depiction is given for the rectangle R, which is obtained through the partial hodograph transformation, i.e. for the (q, p)-variables. This figure suggest that, for particular waves, along any streamline the pressure displays a local minimum at $q = 0$ – equivalently $x = 0$.*

Gathering the results of the above procedure, for different values of constant vorticity, we display the wave height and average depth for maximal waves in Figure 11.

(iii) Linear vorticity

As a last example, we consider the case that vorticity depends linearly on the streamfunction

$$\gamma(-p) = -a_1 p + a_0,$$

then the laminar solution is given by

$$H(p;\lambda) = \int_{p_0}^{p} \frac{1}{\sqrt{\lambda - 2\Gamma(s)}} ds = \int_{p_0}^{p} \frac{1}{\sqrt{\lambda + a_1 s^2 - 2a_0 s}} ds.$$

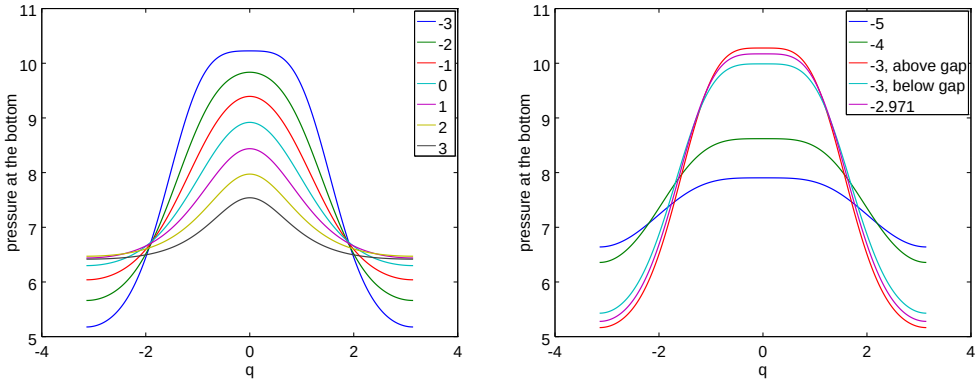

(a) The distribution for waves of maximal amplitude.

(b) The distribution for different values of sub-critical vorticity.

Figure 9: The pressure at the flat bottom for different values of constant vorticity.

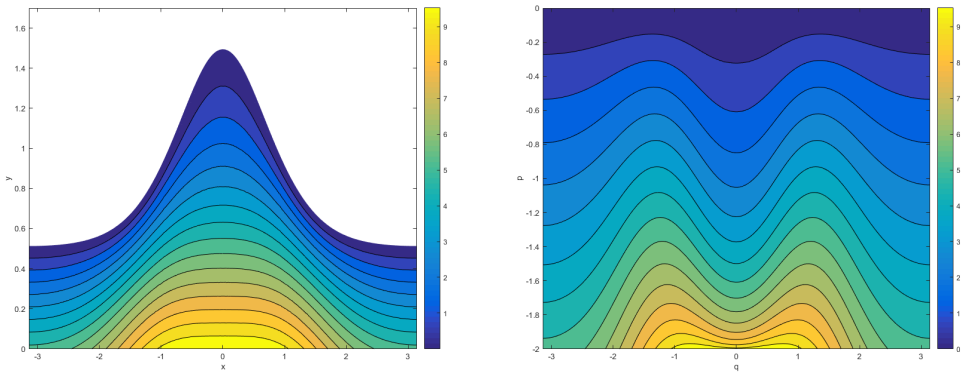

(a) Physical domain.

(b) Fixed domain R obtained through partial hodograph transformation.

Figure 10: The pressure in the interior of the fluid, for the wave obtained at $\gamma = \gamma_{\text{crit}}$ and $Q = Q_G$.

The dispersion relation as given in [34] reads

$$\lambda^* + a_0\sqrt{\lambda^*}F(H(0;\lambda^*) - gF(H(0;\lambda^*)) = 0$$

with

$$F(d) = \frac{\tanh(d\sqrt{1+a_1})}{\sqrt{1+a_1}} \qquad \text{if } a_1 > -1.$$

In [3], we consider $\gamma_\alpha(-p)$ such that $\gamma_\alpha(-p_0) = 0$ and $\gamma_\alpha(0) = \alpha$ for $\alpha = \pm 1$, where we observe that the considered waves display similarities with waves of constant vorticity. The analysis of this particular class of examples was motivated by the discussion in [36], where it is mentioned that, from experiments, wind typically has the effect of producing vorticity in the water near the surface. Thus, we discuss a case of non-constant, continuous distribution of vorticity, which vanishes at the bottom, but not at the surface of the fluid. A more elaborate study on other cases of non-constant vorticity –apart from linear– is performed in [3].

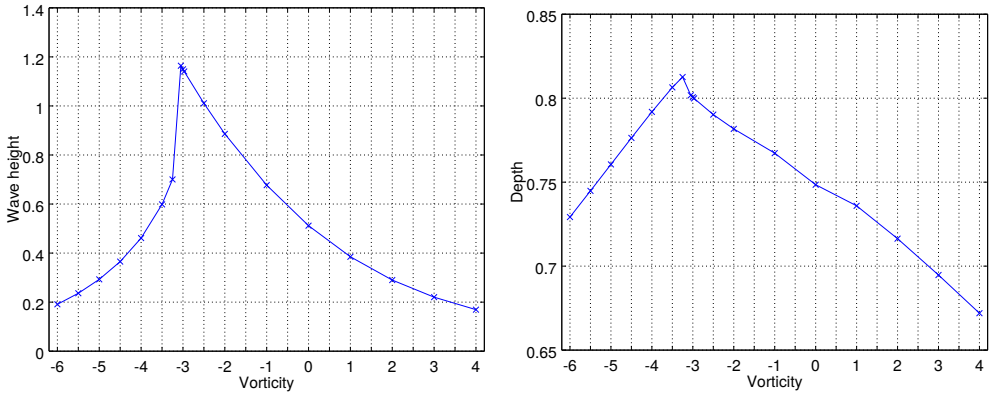

(a) Wave height. (b) Depth

Figure 11: Characteristics of the maximal waves for different values of constant vorticity.

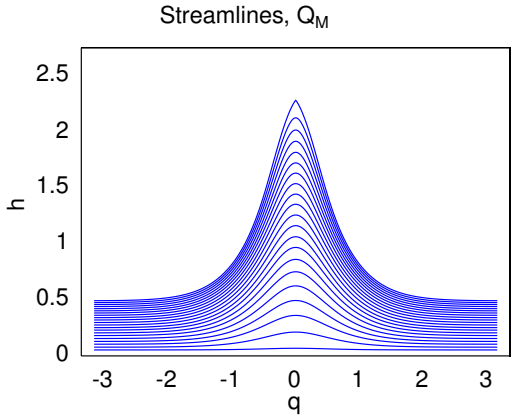

Figure 12: The water wave for linear vorticity $\gamma_\alpha(0) = \alpha = -10$.

Finally, we have computed a wave for which the linear vorticity distribution takes the value $\alpha = -10$ at the free surface and vanishes at the bottom, see Figure 12. For this wave, we observe a different behaviour from the waves of negative constant vorticity $\gamma < \gamma_\ell = -3.062$, with the most striking being the significantly larger wave height and the existence of a stagnation point at the free surface.

Competing Interests. The author declares that he has no competing interests.

Funding. The author was supported by the project *Computation of large amplitude water waves* (P 27755-N25), funded by the Austrian Science Fund (FWF).

Acknowledgements. The author would like to thank A. Constantin and O. Scherzer for the discussion and useful comments on this work. Furthermore, he is thankful to the reviewers for useful comments on the presentation of this work.

References

1. E. L. Allgower and K. Georg, *Introduction to numerical continuation methods*, volume 45, SIAM, 2003.

2. D. Amann and K. Kalimeris, Numerical approximation of water waves through a deterministic algorithm, in preparation.
3. D. Amann and K. Kalimeris, A numerical continuation approach for computing water waves of large wave height, submitted.
4. Y.-Y. Chen, H.-C. Hsu and G.-Y. Chen, Lagrangian experiment and solution for irrotational finite-amplitude progressive gravity waves at uniform depth, *Fluid Dyn. Res.* **42 (4)**, 045511, 2010.
5. D. Clamond, Note on the velocity and related fields of steady irrotational two-dimensional surface gravity waves, *Philos. Trans. Roy. Soc. London A* **370**, 1572–1586, 2012.
6. D. Clamond, New exact relations for easy recovery of steady wave profiles from bottom pressure measurements, *J. Fluid Mech.* **726**, 547–558, 2013.
7. D. Clamond and A. Constantin, Recovery of steady periodic wave profiles from pressure measurements at the bed, *J. Fluid Mech.*, **714**, 463–475, 2013.
8. A. Constantin, The trajectories of particles in Stokes waves, *Invent. Math.* **166**, 523–535, 2006.
9. A. Constantin, On the deep water wave motion, *J of Physics A: Math. and Gen.*, **34(7)** 1405, 2001.
10. A. Constantin, *Nonlinear water waves with applications to wave-current interactions and tsunamis*, CBMS-NSF Conf. Ser. Appl. Math., **81**, SIAM, Philadelphia, 2011.
11. A. Constantin, Estimating wave heights from pressure data at the bed, *J. Fluid Mech.* **743**, R2, 2014.
12. A. Constantin, Extrema of the dynamic pressure in an irrotational regular wave train, *Phys. Fluids* **28** 113604, 2016
13. A. Constantin, M. Ehrnström and E. Wahlén, Symmetry of steady periodic gravity water waves with vorticity, *Duke Math. J.* **140**, 591–603, 2007.
14. A. Constantin and J. Escher, Symmetry of steady periodic surface water waves with vorticity, *J. Fluid Mech.* **498**, 171–181, 2004.
15. A. Constantin and J. Escher, Analyticity of periodic travelling free surface water waves with vorticity, *Ann. Math.* **173**, 559–568, 2011.
16. A. Constantin, K. Kalimeris and O. Scherzer, A penalization method for calculating the flow beneath travelling water waves of large amplitude, *SIAM on Appl. Math.* **75(4)**, 1513–1535, 2015.
17. A. Constantin, K. Kalimeris and O. Scherzer, Approximations of steady periodic water waves in flows with constant vorticity, *Nonlin. Analysis: Real World Appl.* **25**, 276–306, 2015.
18. A. Constantin and W. Strauss, Exact steady periodic water waves with vorticity, *Comm. Pure Appl. Math.* **57**, 481–527, 2004.
19. A. Constantin and W. Strauss, Pressure beneath a Stokes wave, *Comm. Pure Appl. Math.* **53**, 533–557, 2010.
20. A. Constantin, W. Strauss and E. Varvaruca, Global bifurcation of steady gravity water waves with critical layers, *Acta Mathematica* **217(2)**, 195–262, 2016.
21. A. Constantin and E. Varvaruca, Steady periodic water waves with constant vorticity: regularity and local bifurcation, *Arch. Ration. Mech. Anal.* **199**, 33–67, 2011.
22. A.D. Craik, The origins of water wave theory, *Annual review of fluid mechanics* **36**, 2004.
23. A. F. T. da Silva and D. H. Peregrine, Steep, steady surface waves on water of finite depth with constant vorticity, *J. Fluid Mech.* **195**, 281–302, 1988.
24. E. J. Doedel, *Numerical Continuation Methods for Dynamical Systems: Path following and boundary value problems*, chapter Lecture Notes on Numerical Analysis of Nonlinear Equations, pages 1–49, Springer Netherlands, Dordrecht, 2007.
25. M.-L. Dubreil-Jacotin, Sur la détermination rigoureuse des ondes permanentes périodiques d'ampleur finie, *J. Math. Pures Appl.* **13**, 217–291, 1934.
26. J. Escher and B. V. Matioc, Analyticity of rotational water waves, in Elliptic and parabolic equations, *Springer Proc. Math. Stat.* **119**, 111–137, 2015.
27. F. J. von Gerstner, Theorie der wellen, *Ann. Phys.*, **32**, 412–440, 1809.
28. D. Henry, Large amplitude steady periodic waves for fixed-depth rotational flows, *Comm. Partial Diff. Eq.* **38**, 1015–1037, 2013.
29. D. Henry, Steady periodic waves bifurcating for fixed-depth rotational flows, *Quart. Appl. Math.* **71**, 455–487, 2013.
30. D. Henry, Pressure in a deep-water Stokes wave, *J. Math. Fluid Mech.* **13** 251–257, 2011.
31. H.-C. Hsu, Y.-Y. Chen, J. R. C. Hsu, and W.-J. Tseng, Nonlinear water waves on uniform current in Lagrangian coordinates, *J. Nonlinear Math. Phys.* **16 (1)**, 47–61, 2009.
32. I. G. Jonsson, Wave-current interactions, In *The Sea* (Ed. B. Le Méhauté and D. M. Hanes), J. Wiley & Sons, 65–120, 1990.

33. K. Kalimeris, Asymptotic expansions for steady periodic water waves in flows with constant vorticity, *Nonlinear Analysis: Real World Applications* **37**, 182-212, 2017.
34. P. Karageorgis, Dispersion relation for water waves with non-constant vorticity, *European Journal of Mechanics-B/Fluids*, **34**, 7–12, 2012.
35. S. Kassem and H. Özkan-Haller, Forecasting the wave-current interactions at the mouth of the Columbia River, *Proc. 33rd Internat. Conf. Coast. Eng.*, Santander (Spain), 1–6, 1993.
36. J. Ko and W. Strauss, Effect of vorticity on steady water waves, *Journal of Fluid Mechanics*, **608**, 197–215, 2008.
37. J. Ko and W. Strauss, Large-amplitude steady rotational water waves, *European Journal of Mechanics - B/Fluids*, **27(2)**, 96 – 109, 2008.
38. F. Kogelbauer, Recovery of the wave profile for irrotational periodic water waves from pressure measurements, *Nonl. Anal. Real World Appl.* **22**, 219–224, 2015.
39. T. Levi-Civita, Determinazione rigorosa delle onde irrotazionali periodiche in acqua profonda, *Rend. Accad. Lincei*, **33**, 141–150, 1924.
40. T. Lyons, The pressure distribution in extreme Stokes waves, *Nonlinear Anal. Real World Appl.* **31**, 77–87, 2016
41. T. Lyons, The pressure in a deep-water Stokes wave of greatest height, *J. Math. Fluid Mech.* **18**, 209–218, 2016.
42. C.-I. Martin, Dispersion relations for rotational gravity water flows having two jumps in the vorticity distribution, *J. of Math. Anal. and Appl.*, **418 (2)**, 595–611, 2014.
43. C.-I. Martin, Dispersion relations for gravity water flows with two rotational layers, *European J. of Mech. - B/Fluids* , **50**, 9–18, 2015.
44. A. I. Nekrasov, On steady waves, *Izv. Ivanovo-Voznesensk. Politekhn. In-ta*, 3, 1921.
45. K. L. Oliveras, V. Vasan, B. Deconinck, and D. Henderson, Recovering the water-wave profile from pressure measurements, *SIAM J. Appl. Math.* **72**, 897–918, 2012.
46. R. Ribeiro, P.A. Milewski and A. Nachbin, Flow structure beneath rotational water waves with stagnation points, *Journal of Fluid Mechanics* **812**, 792–814, 2017.
47. S. Sastre-Gomez, Equivalent formulations for steady periodic water waves of fixed mean-depth with discontinuous vorticity. *DCDS-A* **37** 2669–2680, 2017.
48. B.L. Segal, D. Moldabayev, H. Kalisch, B. Deconinck, Explicit solutions for a long-wave model with constant vorticity, *Eur. Jour. Mech. - B/Fluids* **65**, 247–256, 2017.
49. G. G. Stokes, On the theory of oscillatory waves, *Trans Cambridge Philos Soc*, **8**, 441–473, 1847.
50. W. Strauss, Steady water waves. *Bul. Am. Math. Soc.*, **47(4)**, 671-694, 2010.
51. D. J. Struik, Détermination rigoureuse des ondes irrotationelles périodiques dans un canal à profondeur finie, *Mathematische Annalen*, **95(1)**, 595–634, 1926.
52. C. Swan, I. P. Cummins and R. L. James, An experimental study of two-dimensional surface water waves propagating on depth-varying currents, *J. Fluid Mech.* **428**, 273–304, 2001.
53. G. P. Thomas, Wave-current interactions: an experimental and numerical study, *J. Fluid Mech.* **216**, 505–536, 1990.
54. M. Umeyama, Eulerian-Lagrangian analysis for particle velocities and trajectories in a pure wave motion using particle image velocimetry, *Philos. Trans. Roy. Soc. London A* **370**, 1687–1702, 2012.
55. E. Varvaruca, Bernoulli free-boundary problems in strip-like domains and a property of permanent waves on water of finite depth, *Proc. Royal Soc. Edinburgh Sect. A: Math.* **138 (6)**, 1345–1362, 2008.